Supporting Information

Salt engineering toward stable cation migration of Na metal anodes

Yingying Ji[a], Hengchao Sun[b], Zhibin Li[a], Liang Ma[a]*, Wanggang Zhang[c], Yiming Liu[c], Likun Pan[d], Wenjie Mai[a] and Jinliang Li[a]*

[a]*Siyuan Laboratory, Guangdong Provincial Engineering Technology Research Center of Vacuum Coating Technologies and New Materials, Department of Physics, Jinan University, Guangzhou, Guangdong 510632, China.*

[b]*Dongguan Power Supply Bureau, Guangdong Power Grid Co., Ltd, Dongguan 523000, People's Republic of China.*

[c]*College of Environmental Science and Engineering, Taiyuan University of Technology, Taiyuan 030024, People's Republic of China.*

[d]*Shanghai Key Laboratory of Magnetic Resonance, School of Physics and Electronic Science, East China Normal University, Shanghai 200241, China.*

**Corresponding author: maliang2415@jnu.edu.cn (Liang Ma); lijinliang@email.jnu.edu.cn (Jinliang Li)*

Experimental Section

1. Preparation of electrolytes and electrodes

The electrolytes were prepared by dissolving a certain amount of the potassium bis(fluorosulfonyl)imide (KFSI) salt, sodium bis(fluorosulfonyl)imide (NaFSI) salt, KPF_6 or $NaPF_6$ into the mixed solvent of EC/PC (1:1, in vol), including a blank electrolyte (pure EC/PC), KFSI (1 M KFSI in EC/PC), NaPF (1 M $NaPF_6$ in EC/PC), KPF (1 M KPF_6 in EC/PC), NaFSI (1 M NaFSI in EC/PC), NaPF-K (5% KFSI into NaPF), NaPF-KPF (5% KPF into NaPF) and NaPF-FSI (5% NaFSI into NaPF), respectively. For the preparation of the Na metal anode, the electrode of metal Na was made by pressing and then cutting to a disc directly with a diameter of 14 mm. All the electrolytes and electrodes were obtained in an Ar-filled glove box with oxygen and moisture levels less than 0.1 ppm. Carbon cloth (CC) was used to assemble asymmetric cells. The $Na_3V_2(PO_4)_3$ (NVP) cathode was provided by Guangzhou Great Power Energy & Technology Co., Ltd.

2. Electrochemical tests

All the electrochemical tests were carried out in CR 2032 coin cells with glass fiber as the separator. For Na||Na symmetric cells, the Na stripping and deposition process was performed by a battery test system (Neware BTS-4000) for 1 h at a current density of 0.5 mA cm^{-2}. The Na||CC asymmetric cells were assembled to evaluate the Coulombic efficiencies (CE) for 1 h at a current density of 0.5 mA cm^{-2} with a cutoff voltage of 1 V. For the nucleation overpotential analysis, symmetric Na||Na cells were fabricated with a current density of 0.5 mA cm^{-2}. The Na||NVP full cells were cycled in the potential window between 2.5 V and 3.7 V at a current density of 50 mA g^{-1}. Electrochemical impedance spectra (EIS) were carried out on an electrochemical workstation (Princeton STAT 3400) and recorded from 10 kHz to 0.01 Hz with a bias voltage of 10 mV.

3. Characterizations

The solvated structures of electrolytes were confirmed by Raman spectroscopy

(Horiba, T64000) using a 532-nm emission line of a pulsed laser and FTIR spectra (Nicolet, Nexus 670) attenuated total reflectance mode. The morphology information was performed by a metallographic microscope (Leica). The structures of electrodes were confirmed by XRD (D8 Rigaku9000). The surface features were recorded by X-ray photoelectron spectroscopy (XPS, Thermo Fisher Scientific, K-Alpha).

4. DFT computational methods

The density functional theory (DFT) computations were performed using the Vienna ab initio simulation package (VASP). The Perdew-Becke-Ernzerhof (PBE) functional and projector augmented wave (PAW) scheme were adopted for geometric optimizations. An energy cutoff of 500 eV for the plane wave basis set was used for the structure optimization and static self-consistent. All structures were optimized with a convergence criterion of 1×10^{-4} eV for the energy and 0.05 eV/Å for the forces. For the Na metal anode/electrolyte interface calculations, the Na (001) surface was chosen for the Na-metal/electrolyte modeling. A 3×3×1 k-point mesh was used for the Brillouin zone sampling. The energy of bond cleavage (E_{BC}) of different anions (FSI^- and PF_6^-) at the Na metal/electrolyte interface was calculated as follows: $E_{BC} = E_{ADS}-E_{SPE}$, where E_{ADS} was adsorption energy of the anion at the Na surface, E_{SPE} was the single point energy of the F atom after bond cleavage. For the bond binding energy of cations (K^+ or Na^+) and anions (FSI^-) calculations, a 3×3×3 k-point mesh was used for the Brillouin zone sampling. The binding energy (E_{BE}) of the K^+-FSI^- or Na^+-FSI^- was calculated as follows: $E_{BE} = E_{total}-E_{cation}-E_{anion}$, where E_{total} was the total energy of the K^+-FSI^- or Na^+-FSI^-, E_{cation} was the energy of K^+ or Na^+, E_{anion} was the energy of FSI^- , respectively.

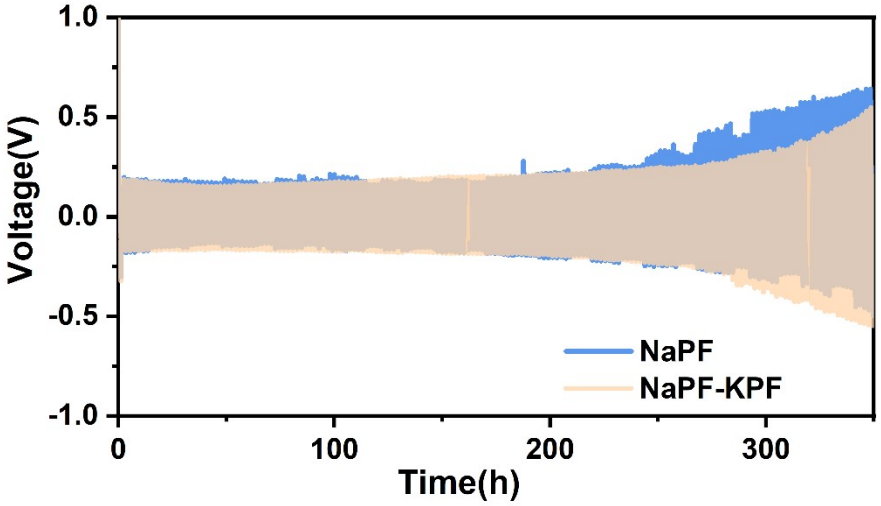

Figure S1. Electrochemical performance of Na||Na symmetric cells in NaPF-KPF electrolyte.

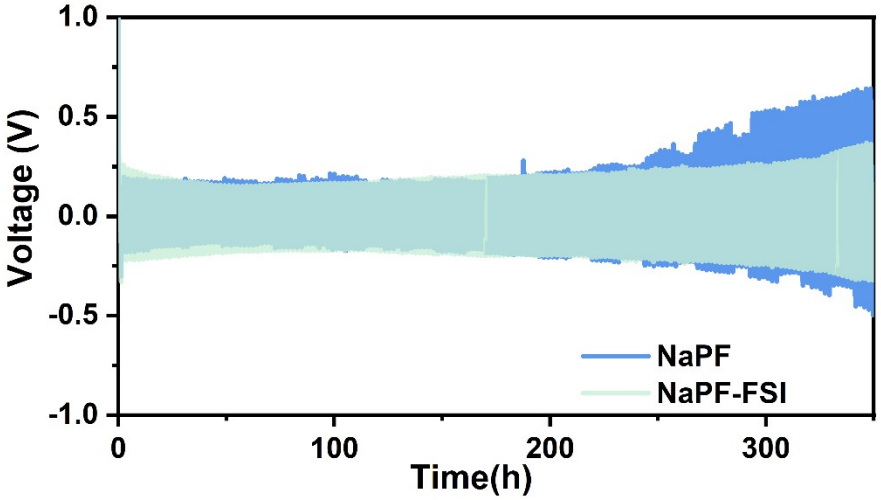

Figure S2. Electrochemical performance of Na||Na symmetric cells in NaPF-FSI electrolyte.

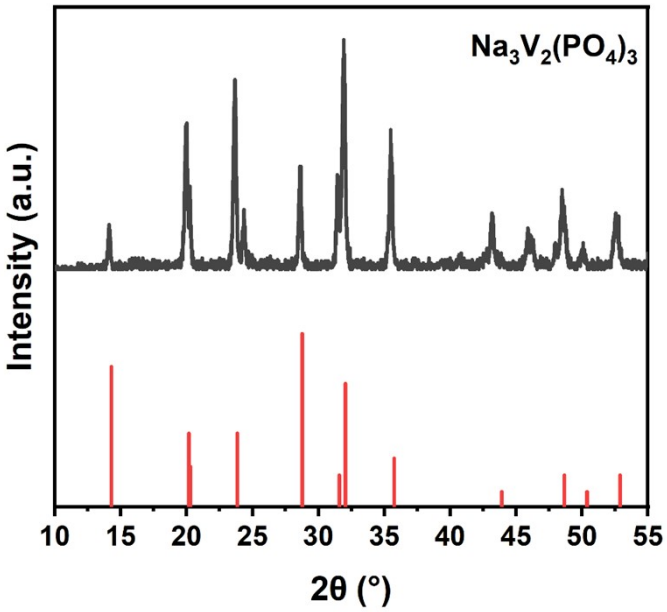

Figure S3. XRD spectrum of NVP.

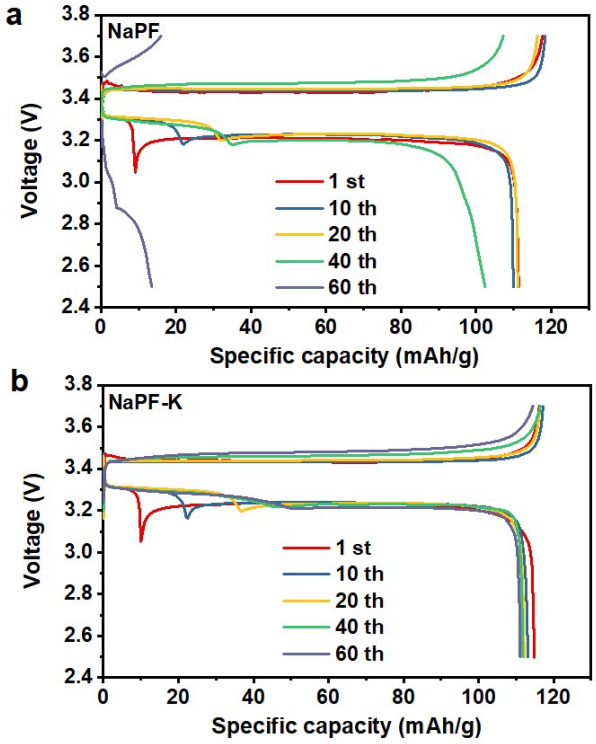

Figure S4. The charge-discharge curves of the Na||NVP full cells in (a) NaPF electrolytes and (b) NaPF-K electrolytes.

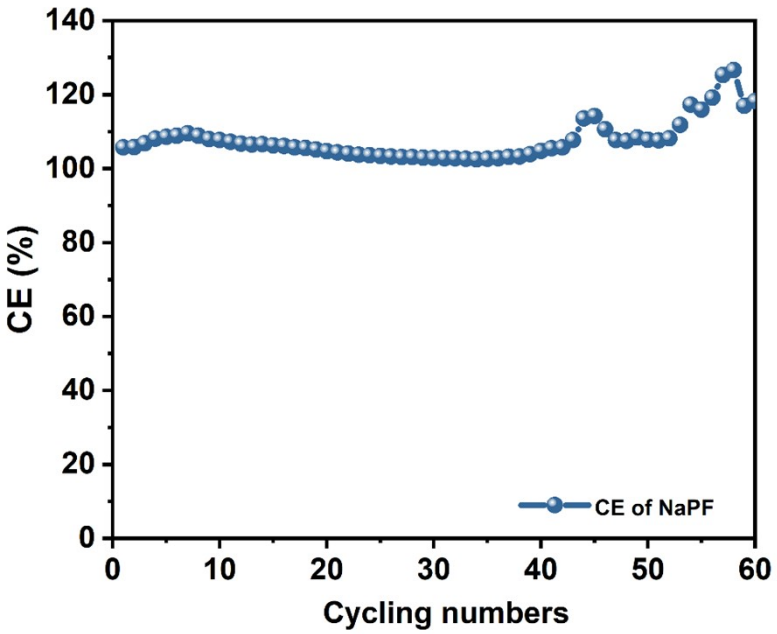

Figure S5. CE of Na||NVP full cells in NaPF electrolyte.

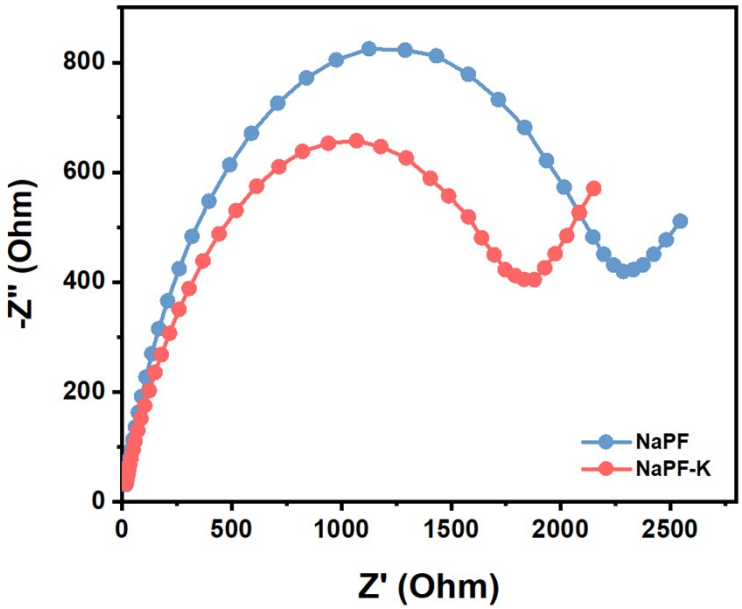

Figure S6. The Nyquist plots of Na||Na symmetric cells in NaPF electrolyte and NaPF-K electrolyte.

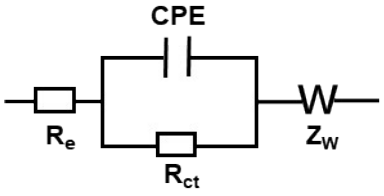

Figure S7. The equivalent circuit of the above Nyquist plot.

The Nyquist plots are composed of a semicircle in the high frequency regions and a sloping line in the low-frequency region, which an equivalent electric circuit can well fit (shown in the inset of Figure S7), where the R_e denotes the electrolyte resistance. The R_{ct} and CPE are the charge transfer resistance and the associated double-layer capacitance. The Z_w is referred as the ion diffusion resistance in the solution, also known as Warburg impedance.

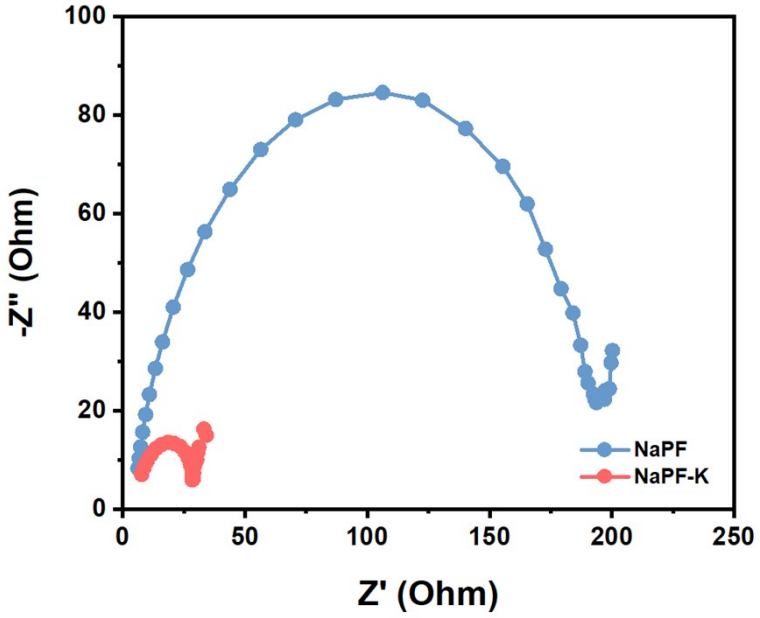

Figure S8. The Nyquist plots of Na||CC asymmetric cells in NaPF electrolyte and

NaPF-K electrolyte.

The interfacial resistance of asymmetric cells with NaPF electrolyte is 193 Ω and the resistance of asymmetric cells with NaPF-K electrolyte decreases to 28 Ω.

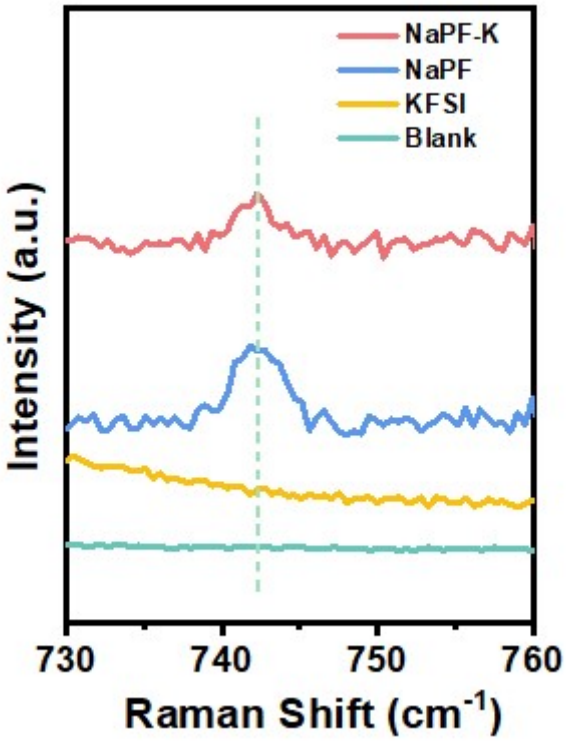

Figure S9. The enlargement of the $NaPF_6$ characteristic peak.

The peaks associated with the anion of the Na^+ salt will show a red shift due to the reduced coordination between cation and anion and increased coordination between cation and solvent.[1] The peak of the Na^+-PF_6^- in the NaPF-K electrolyte shows a smaller shift than that in the NaPF electrolyte (Figure S9). This result indicates that the addition of KFSI has a weak effect on the Na^+-PF_6^- ion pair.

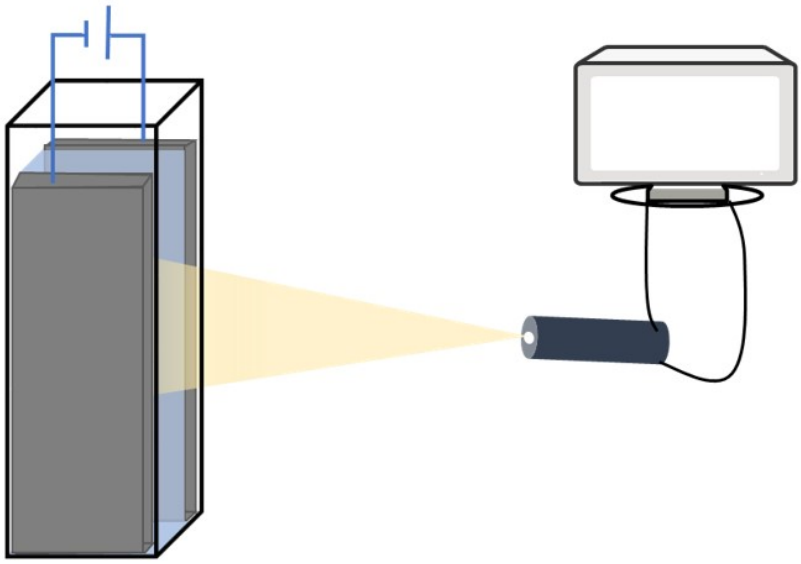

Figure S10. Schematic of in-situ optical microscope observation device.

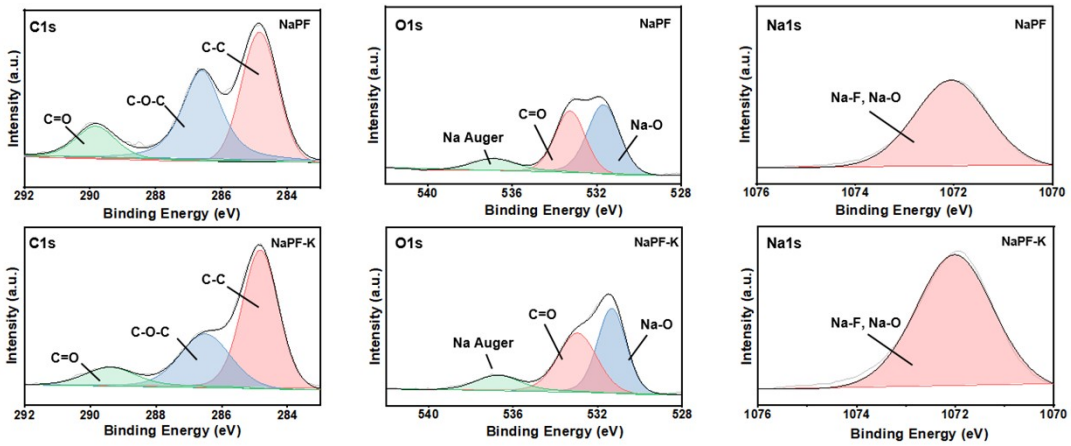

Figure S11. The composition analysis of the SEI layer derived from NaPF and NaPF-K electrolyte by XPS: C 1s, O 1s and Na 1s high-resolution XPS spectra.

For the NaPF electrolyte, the SEI layer mainly consists of various organic species due to the reaction between electrolyte and electrode during cycling, and the SEI layer for the NaPF-K electrolyte consists of inorganic compounds such as NaF and KF.

Therefore, for NaPF-K electrolytes, the C and O contents decrease due to the reduced decomposition of electrolytes, while the F and Na contents increase significantly.

Reference:

S1. J. Holoubek, H. Liu, Z. Wu, Y. Yin, X. Xing, G. Cai, S. Yu, H. Zhou, T. A. Pascal, Z. Chen and P. Liu, *Nat Energy*, 2021, **6**, 303-313.